Full-scale reinforced embankment on deep jet mixing improved ground

Y. P. LAI, D. T. BERGADO, G. A. LORENZO and T. DUANGCHAN
Geotechnical and Geoenvironmental Engineering Programme, School of Civil Engineering, Asian Institute of Technology, Thailand

A 6 m high reinforced embankment constructed on deep-mixing improved soft Bangkok clay is presented. The jet mixing method with cement slurry employing a jet pressure of 20 MPa was utilised in the installation of deep mixing piles. Surface settlements and lateral movements were monitored during and after construction. The deep mixing improvement has effectively reduced the settlement by as much as 70%. The differential settlement between pile and soil ranged from 8 to 20% of the average settlement. Moreover, the back analysis confirmed the laboratory investigation that the soil–cement pile installed by jet mixing can have a higher after-curing void ratio and, consequently, higher permeability and coefficient of consolidation. Finally, the higher permeability ratios, $K_{v,p}/K_{v,c}$, of 30 and 40 were confirmed from numerical and analytical back analyses, respectively.

Keywords: analytical back analysis; deep cement mixing; reinforced test embankment; soft clay

Une berge renforcée de 6 m de hauteur, construite sur une argile tendre de Bangkok améliorée par mixage profond fait l'objet de cette étude. Nous avons utilisé la méthode de mixage par injection de ciment liquide, sous une pression de 20 MPa, dans l'installation de piles à mixage profond. Les affaissements de surface et les mouvements latéraux ont été suivis pendant et après la construction. L'amélioration par mixage profond a effectivement réduit de 70% l'affaissement. L'affaissement différentiel entre pile et sol représente 8 à 20 % de l'affaissement moyen. De plus, la rétro-analyse a confirmé l'étude en laboratoire montrant que la pile sol-ciment installée par mixage à injection peut avoir un taux de pore plus élevé après cuisson et, en conséquence, une perméabilité et un coefficient de consolidation plus élevés. Enfin, des taux plus élevés de perméabilité, $K_{v,p}/K_{v,c}$, de 30 et 40, ont été confirmés par les rétro analyses numériques et analytiques respectivement.

Introduction

Ground improvement by cement stabilisation can broadly be divided into shallow stabilisation and deep stabilisation. Shallow stabilisation, which includes stabilisation of subgrade for roadways and airfields and other similar structures, normally employs 'low water content' mixing. The deep stabilisation, on the other hand, includes deep mixing method (DMM) using either slurries or cement powder to form columns of improved soil in the ground. The improved column of soil is considered to act as reinforcement or as a pile, transferring the load to the skin and to the bottom-end of the improved column of soil. The methods of mixing are broadly divided into two: either mechanical mixing or high-pressure jet mixing (Kamon and Bergado, 1991; Kamon, 1996; Porbaha, 1998). In the mechanical mixing the chemical admixtures are mixed into the soil by mixing blades, while in the jet mixing the same are mixed into the soil through a water jet or slurry admixture. The slurry deep mixing and jet mixing methods would normally produce high water content cement-admixed clay; furthermore, the soft clay deposit normally has high water content.

The technique of reinforcing earth has been extensively used in the construction of earth-retaining walls and embankment slopes, and in the stabilisation of embankments placed on soft ground. The reinforced soil mass is generally called mechanically stabilised earth (MSE). MSE structures can be divided into three main parts: (*a*) facing elements, which act as an armour to prevent erosion of retained, fill materials; (*b*) reinforcing elements, which add tensile strength in the soil mass; (*c*) engineering fill, which makes the bulk of the structure.

A full-scale deep mixing improved soft clay foundation supporting a 6 m high reinforced embankment was constructed within the soft Bangkok clay area in Thailand, and it was monitored in order to study its consolidation and deformation behaviour. The jet mixing technique having a jet pressure of 20 MPa was utilised in the installation of deep mixing piles. Based on the results of the instrumentation of this full-scale test, the compression mechanism of deep mixing pile-improved ground overlain by a reinforced embankment is discussed in this paper.

Test embankment on soft ground improved with DMM

Site and description of the test embankment

A 6 m high test embankment reinforced with polyvinyl chloride (PVC)-coated hexagonal wire mesh reinforcement

(GI 5240) Paper received 24 March 2005; last revised 29 March 2006; accepted 3 July 2006

was constructed at Wangnoi District, Ayuthaya, Thailand (Bergado *et al.*, 2002). The foundation soils and their properties at the site of the test embankment are shown in Fig. 1. Prior to embankment construction, the monitoring instruments were installed and the foundation subsoil was then improved with soil–cement columns, which were installed in situ by a jet mixing method employing a jet pressure of 20 MPa. Soil–cement piles were installed at 1·5 m spacing in a square pattern, except for the perimeter soil–cement piles which were installed at 2·0 m spacing (Figs 2(a) and (b)). The water–cement ratio (w/c) of the cement slurry and the cement content employed for the construction of deep mixing piles were 1·5 and 150 kg/(m^3 of soil), respectively. Each deep mixing pile has a diameter of improvement of 0·5 m and a length of 9·0 m, penetrating down to the bottom of the soft clay layer, as shown in the section view of the embankment (Fig. 2(b)). The deep mixing piles were allowed to cure while the dissipation of excess pore water pressure was monitored until about 80 days prior to the embankment construction (Bergado *et al.*, 2002).

The embankment was made of well-compacted silty sand backfill reinforced with PVC-coated hexagonal wire mesh. The backfill soil had a compacted unit weight of 18·20 kN/m^3, a drained cohesion of 7·70 kPa, a drained angle of internal friction of 22° and a maximum dry density and optimum water content of 16·1 kN/m^3 and 15% respectively. During construction, the embankment filling was done at 0·375 m lift thickness and was compacted to at least 98% of the maximum dry density of the fill material (Bergado *et al.*, 2002). To support the vertical side of the embankment, concrete facing with dimensions of 1·50 m × 1·50 m × 0·15 m were installed, each being held by two layers of hexagonal wire mesh reinforcements, resulting in a vertical spacing of the reinforcements of 0·75 m (Fig. 2(b)). All reinforcements were 4 m long and were laid horizontally behind the concrete facing. The finished embankment was 6 m high. The embankment construction was completed within 15 days: it started on 28 January 2002 and ended on 12 February 2002.

Effect of jet mixing on the surrounding soil

Excess pore water pressure was developed in the foundation soil during the installation of deep mixing piles by jet mixing method employing a jet pressure of 20 MPa. The excess pore pressures in the foundation soils at 3 m and 6 m depths after installation of deep mixing piles are shown in Figs 3 and 4 respectively. The piezometers installed outside but near the improved foundation at 3 m depth were designated as p1/3, p2/3, p3/3, p4/3, and p5/3 in Fig. 3, while those installed within the improved ground were designated as p6/3, p7/3, and p8/3 (refer to Figs 2(a) and 2(b) for the locations of these piezometers). Similarly, the piezometers installed outside but near the improved foundation at 6 m depth were designated as p1/6, p2/6, p3/6, p4/6, and p5/6 in Fig. 4, while those installed within the improved ground were designated as p6/6, p7/6, and p8/6. The data indicated that there was relatively higher excess pore pressure build-up at 6 m depth than at 3 m depth, and this trend was observed both within and outside the improved foundation. Therefore, the development of excess pore water pressure was affected by the overburden pressure, and it tended to be higher at deeper depths. The average excess pore pressures just after the installation were 9·2 kPa and 27 kPa at 3 m and 6 m depth within the improvement zone respectively. After 70 days of dissipation, these excess pore pressures decreased to 1·6 kPa and 8·3 kPa respectively.

Furthermore, Fig. 4 demonstrated that higher excess pore pressure was developed at points located within the improved foundation than at those points outside the improvement zone at 6 m depth; however, this phenomenon was not

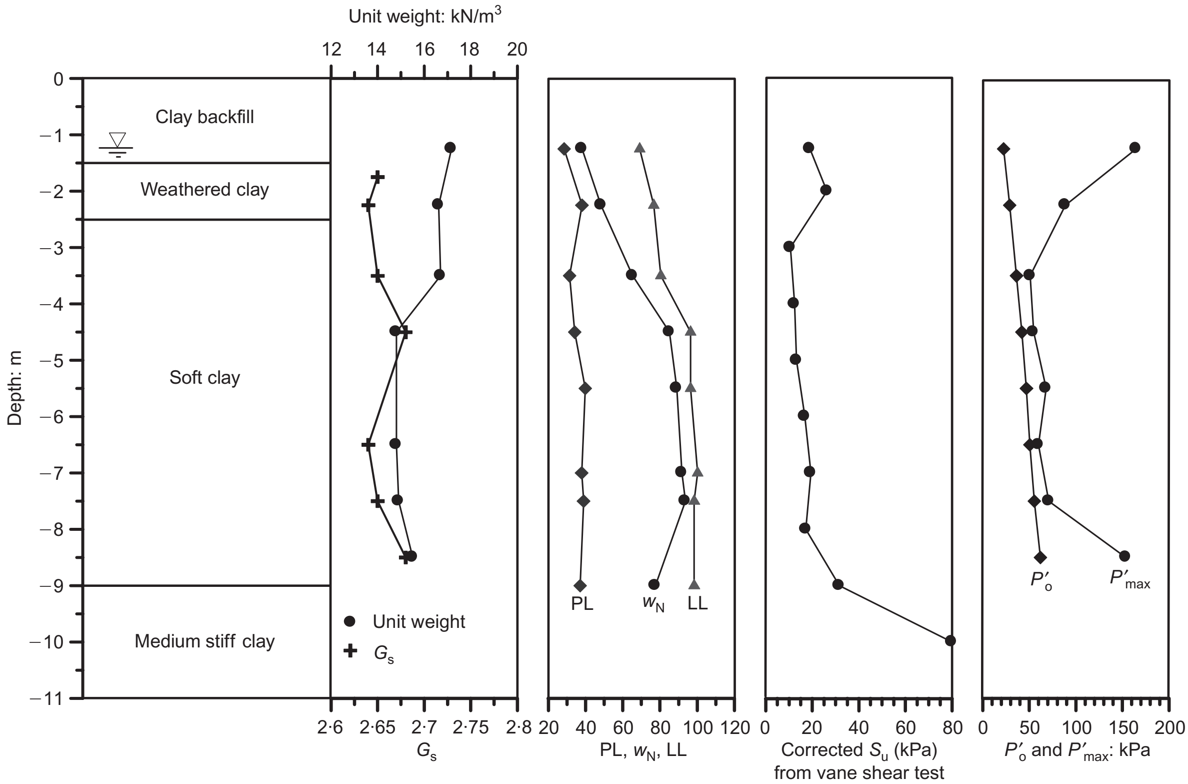

Fig. 1. Soil profiles under the hexagonal wire reinforced test embankment: G_s, specific gravity; PL, plastic limit; w_N, natural water content; LL, liquid limit; S_u, undrained shear strength; P'_o, overburden effective stress; P'_{max}, the maximum past pressure

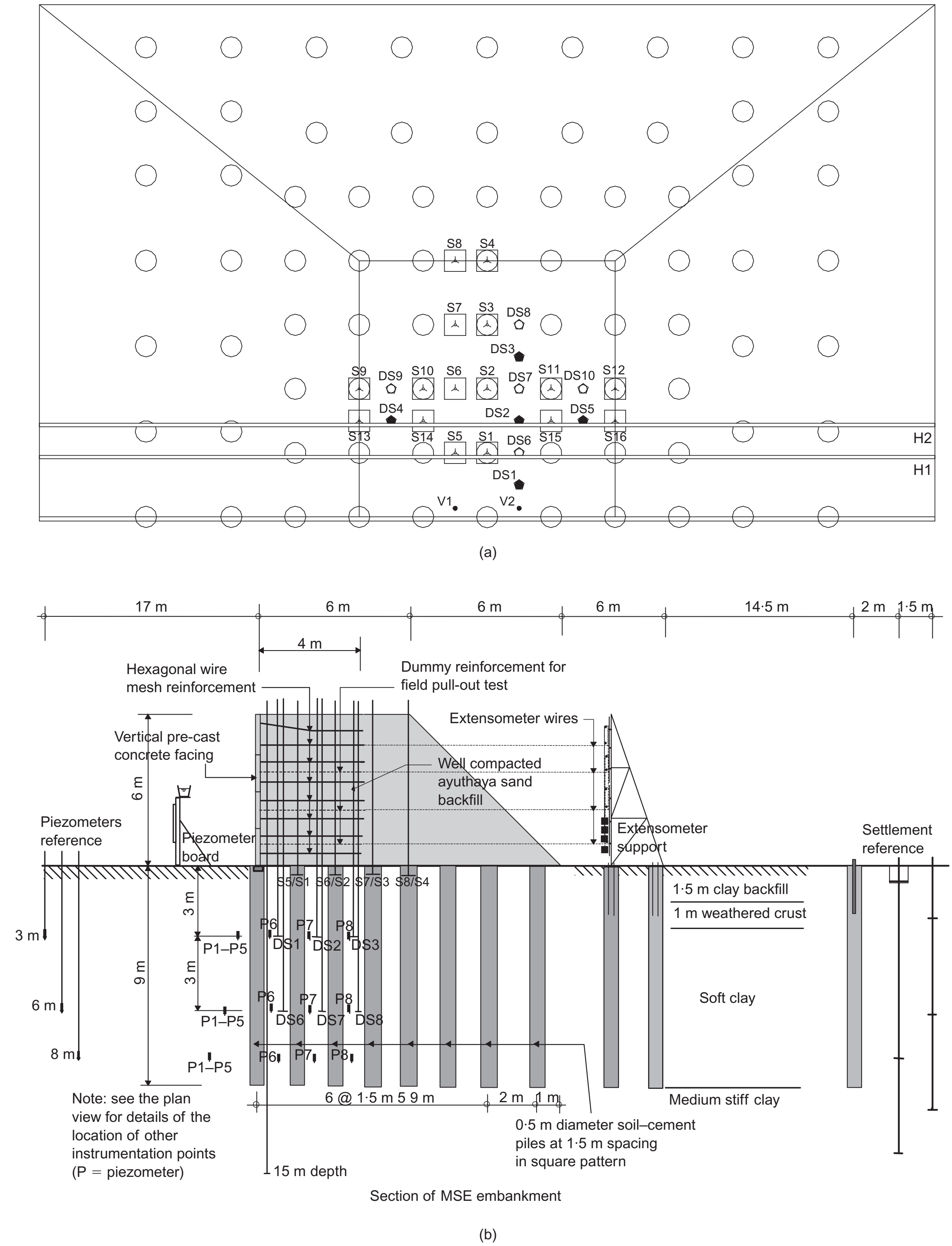

Fig. 2. (a) Plan view of the test embankment on DMM piles showing the locations of surface settlement plates (S) and deep settlement plates (DS). (b) Centreline elevation of the test embankment on deep mixing piles

obvious at 3 m depth, as shown in Fig. 3. The latter observation is indicative that the jet of water during jet mixing operation must have traversed a wider distance at shallower depth, thereby causing higher excess pore water pressure even to those points located at the proximity of the improvement zone as demonstrated by the piezometers installed near the perimeter of the improvement zone. This development of excess pore water pressure eventually could reduce the bearing capacity of the nearby foundation and, hence, may lead to excessive settlement and even collapse of the existing structure.

Pullout resistance of PVC-coated hexagonal wire mesh reinforcement

A pullout test was conducted using a 1270 mm × 762 mm × 508 mm pullout box made of steel plates and steel channels. The silty sand backfill was compacted by hand

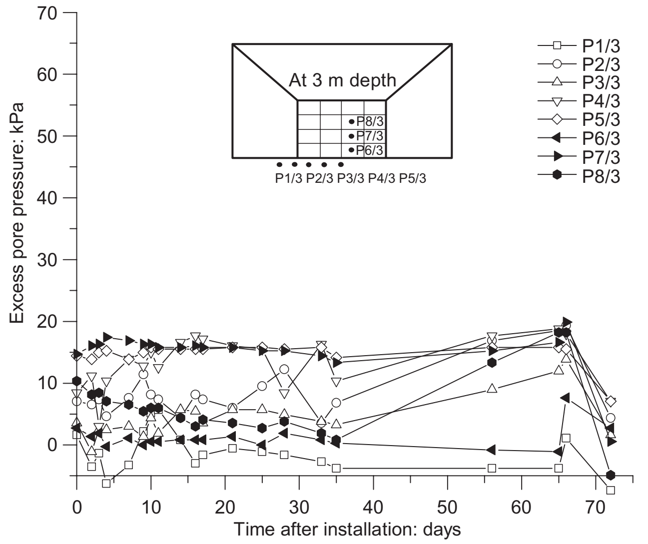

Fig. 3. Excess pore pressure at 3 m depth after installation of deep mixing piles by the jet mixing method

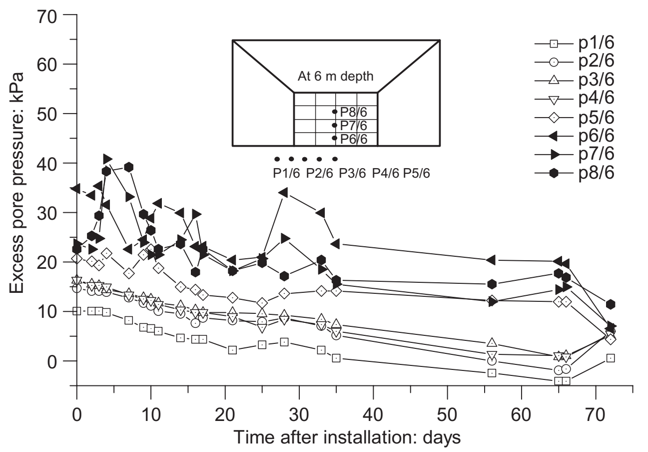

Fig. 4. Excess pore pressure at 6 m depth after installation of deep mixing piles by the jet mixing method

operated electric vibrator to at least 90% of maximum dry density. The laboratory pullout tests under various normal pressures of PVC-coated hexagonal wire reinforcement utilised in the test embankment are shown in Fig. 5 (Duangchan, 2002). The pullout resistance values shown in the figure corresponded to a reinforcement embedment length of 0·9 m. Obviously, the pullout resistance increases with increasing normal pressure, but the corresponding maximum pullout displacement decreases with increasing normal pressure. The pullout resistances corresponding to normal pressures of 27, 54, 81 and 105 kPa are 35·6, 50·3, 58·7 and 66·5 kN/m respectively.

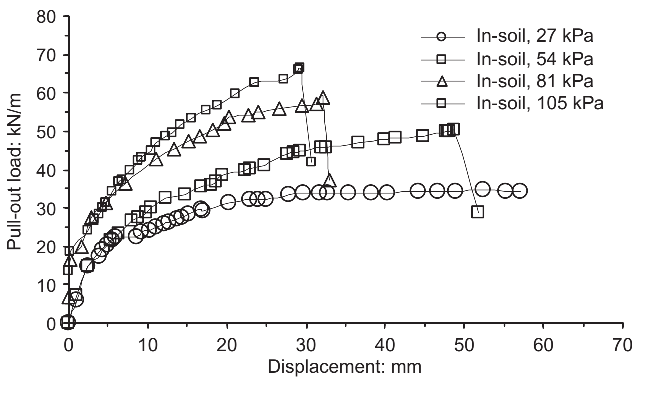

Fig. 5. Laboratory pullout resistance of PVC-coated hexagonal wire reinforcement (after Duangchan, 2002)

Settlement behaviour of soil–cement piles improved soft clay foundation

Figure 6 shows the settlements on top of deep mixing piles and on the surface of surrounding clay during and after construction up to one year of full embankment loading. From these actual observed data, the average settlements on deep mixing pile and on clay amounted to about 122 and 162 mm respectively, after embankment construction. One year after embankment construction, the average settlements on deep mixing pile and on clay amounted to about 285 and 335 mm respectively. The corresponding average settlement at the bottom of the reinforced soil is, therefore, approximately 310 mm one year after embankment construction. Using the method of Asaoka (1978), the average total settlements of deep mixing pile and of the surrounding soil were predicted as shown in Fig. 7 using the data recorded from settlement plates S11 and S15, which demonstrated the average settlement of the deep mixing piles and the surrounding soil respectively. The maximum total settlements of deep mixing pile and of the surrounding soil amounted to 340 and 440 mm respectively. Thus, about 40% of the total settlement occurred during the construction of the test embankment.

Moreover, if there had been no improvement in the foundation soil, the settlement of embankment one year after construction could have been greater than 1000 mm (Bergado and Lorenzo, 2003). Thus, the embankment load (weight of embankment) has been transferred to the deep mixing piles, thereby not only reducing the intensity of pressure on the surrounding clay, and therefore the magnitude of its settlement, but also increasing the bearing capacity of the improved foundation. The deep mixing piles

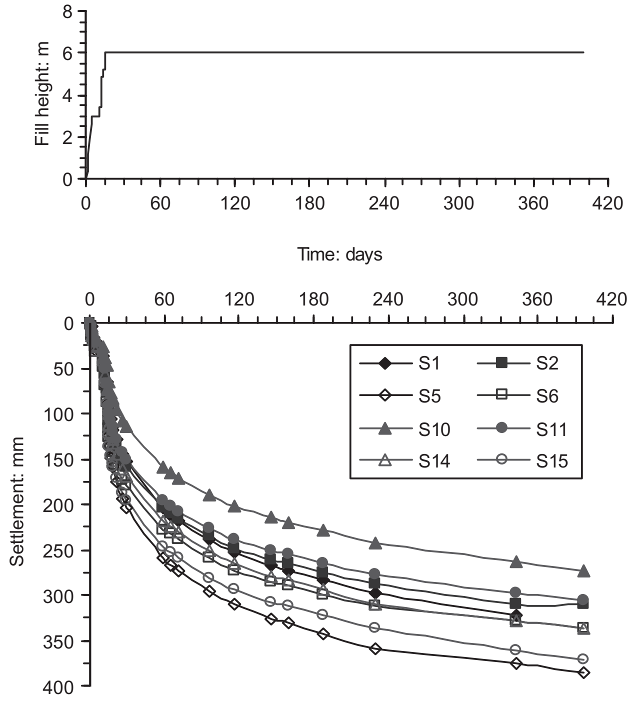

Fig. 6. Surface settlement 'on clay' and 'on piles' near the centre of test embankment (solid symbols: on piles; hollow symbols: on clay)

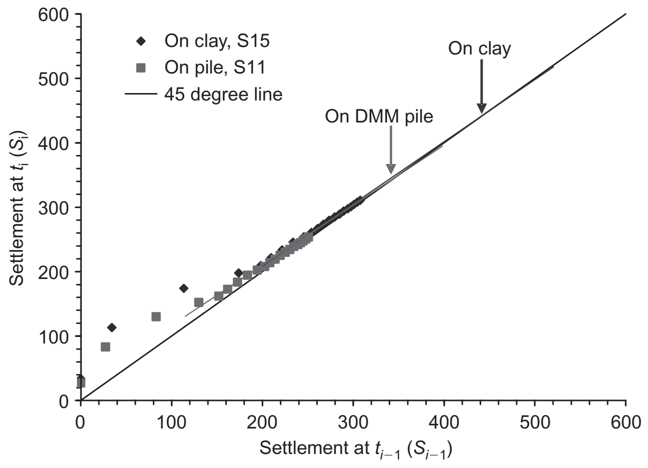

Fig. 7. Prediction of total settlement using Asaoka's observational method

have, therefore, transferred the load down to their bottom ends and, consequently, affected a settlement reduction in the soft clay foundation by about 70%.

The deep mixing piles also promoted a faster rate of consolidation of the improved foundation. The consolidation settlement of the improved ground was almost 90% one year after construction, as can be calculated from the predicted total settlement and the settlement after one year. For settlement plates, S11 and S15 (see Fig. 6), for example, the settlement of pile and clay were 298 and 362 respectively, one year after embankment construction; hence, the corresponding degree of consolidation of the improved ground was, on average, approximately 86%. If there had been no improvement in the 6·5 m thick soft clay (Figs 1 and 2(b)), the 90% consolidation settlement could have been attained only after 9 years post-construction (assuming actual coefficient of consolidation of soft clay, $C_v = 4\ m^2/year$ from back analysis). Moreover, the time–settlement plot obtained from deep settlement plates installed at 3 m and 6 m depth (Fig. 8) also confirmed the faster rate of consolidation settlement of the deep mixing improved ground. Figure 8 demonstrated that both settlements at the surface, at 3 m depth and at 6 m depth indicated the same pattern of consolidation behaviour, which implied that the rate of consolidation was almost uniform over the entire depth of improvement owing to the presence of deep mixing piles.

Local differential settlement between deep mixing pile and surrounding clay

The local differential settlements between pile and adjacent clay range from 25 mm to 60 mm (Fig. 6) when the average settlement of deep mixing piles amounted to 285 mm after one year of full embankment loading. This implies that the local differential settlement between the deep mixing pile and the surrounding clay under the hexagonal wire reinforced embankment can range from 8 to 20% of the average settlement. This amount of local differential settlement was, however, almost eliminated at the surface of embankment owing to the combined effect of compaction as well as reinforcement stiffness and arching of overlying reinforced soil. Significantly, Fig. 6 also demonstrates that the magnitude of local differential settlements between piles and surrounding clay had been almost fully attained after just one month of full embankment loading. This practically implies that, for a road embankment constructed on deep mixing piles, the final surfacing could better be done at least one month after embankment construction, allowing time to compensate for the differential settlement.

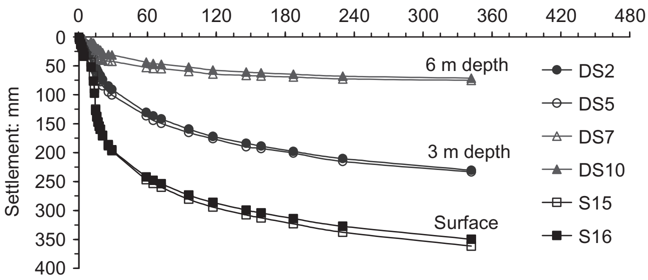

Fig. 8. Comparison of settlements at designated depths below the embankment

Lateral movement behaviour of embankment and improved soft foundation soil

The lateral movement profiles of the improved foundation soils as well as the wall facing of the reinforced embankment are shown together in Fig. 9. The maximum measured lateral movements in the foundation subsoil after embankment construction and 7 months after embankment construction amounted to 5 mm and 45 mm respectively, and both of them occurred at approximately 3·5 m depth below the surface of clay backfill where the weakest zone of soft clay layer (Fig. 9, Fig. 1) was found. Since the average settlement on clay amounted to 162 mm and 325 mm after embankment construction and 7 months after embankment construction, respectively, these magnitudes of lateral movement were only 3 and 14% of the corresponding vertical settlement of the embankment.

In addition, the top of the vertical facing experienced a forwards movement of only 30 mm after embankment construction; it increased afterwards, amounting to 230 mm after 7 months. The time-dependent behaviour of the lateral movement of the wall is attributed to the time-dependent lateral movement of the foundation soil as well as the time-dependent rotation of the embankment body owing to uneven consolidation settlement of the improved foundation soil. From Fig. 9, the bottom of the embankment just after construction underwent translational movement of 16 mm; thus, for the 30 mm forwards movement at the top of the vertical facing just after construction, the remaining 14 mm movement could be attributed to the consequent forwards movement of the precast concrete-facing panel as a result of the mobilisation and subsequent elongation of hexagonal wire reinforcements. After 7 months the lateral (forwards) movement at the bottom of the embankment amounted to 90 mm; and this translational movement is caused by the horizontal thrust of the sloping side of the embankment. Moreover, after 7 months the embankment underwent rotation, resulting from the uneven consolidation settlement of the foundation soil as shown in Fig. 9. The gradient of the settlement profile at the bottom of embankment after 7 months, as can be interpreted from Fig. 10, is approximately 0·02; or simply 20 mm vertical per meter horizontal. Assuming that the reinforced portion of the embankment after construction behaved rigidly after mobilising the pullout resistance of the reinforcements, this rotation would consequently cause an additional forward movement at the top of the 6 m high embankment of 120 mm. Thus, after 7 months, the lateral movement at the top of the vertical facing is estimated to consist of: 14 mm owing to mobilisation and

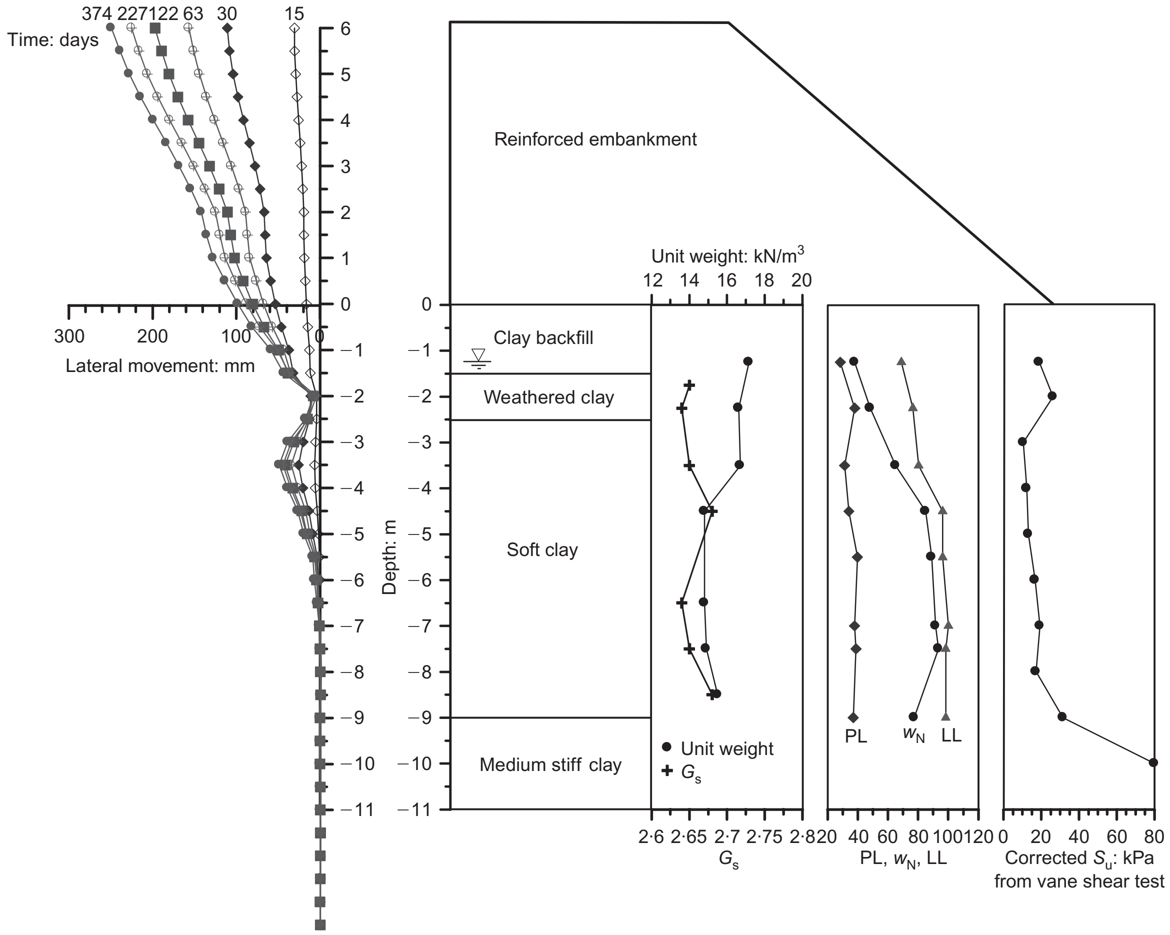

Fig. 9. Lateral movement profile with time of the foundation soils and wall facing

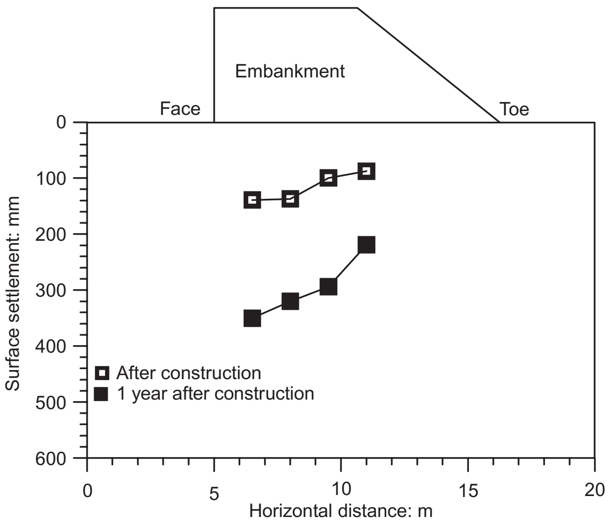

Fig. 10. Settlement profile under the embankment

elongation of reinforcements, plus 90 mm translational movement of the embankment body, plus 120 mm owing to the rotation of the embankment body, which yielded a total magnitude of 224 mm. This estimated lateral movement of 224 mm at the top of the vertical facing agrees with the measured value of 230 mm. The slight underestimation of the estimated lateral movement could be attributed to the subsequent effect of rotation of the embankment that might have increased slightly the horizontal thrust of the soil in the reinforced zone and, thus, increased the elongation of the reinforcements. Therefore, the time-dependent lateral movement of the vertical facing was greatly affected by the unsymmetrical configuration and loading of the embankment and the consequent uneven consolidation settlement of the foundation soil.

Analytical and numerical back analysis of the rate of settlement

To obtain the basic consolidation properties of DMM piles installed by jet mixing method, analytical and numerical simulations of the observed settlement of the test embankment were performed. The analytical simulation was done using the technique of Lorenzo and Bergado (2003a) for the consolidation analysis of deep mixing improved ground, together with Asaoka's observational method to estimate the total settlement (Asaoka, 1978); while the numerical simulation was performed using a finite element (FE) method with PLAXIS version 7 software.

Analytical model for the rate of settlement of deep mixing improved ground

To calculate the average degree of consolidation of the soil–cement pile improved ground, the following modified time factors obtained from the analytical model of Lorenzo and Bergado (2003a) must be substituted to the standard solution (or chart) or to any approximate solutions (e.g., Sivaram and Swamee, 1977) of the one-dimensional consolidation equation. These are given as: equal stress condition between DMM pile and soil

$$T_{v,\sigma} = \left(\frac{(m_{v,p}/m_{v,c})}{(m_{v,p}/m_{v,c}) + (n^2 - 1)(C_c/C_s)_p} \right) \left(\frac{c_{v,p}t}{H_p^2} \right) \quad (1)$$

and equal strain condition between DMM pile and soil

$$T_{v,\varepsilon} = \left(\frac{1}{1 + (n^2 - 1)(C_c/C_s)_p} \right) \left(\frac{c_{v,p}t}{H_p^2} \right) \quad (2)$$

where
$(C_c/C_s)_p$ is the ratio of the compression and swelling indices of the DMM pile at stress level corresponding to the loading condition (if the DMM pile does not reach to its yield stress, this constant can be taken as unity); $c_{v,}$ is the coefficient of consolidation of the DMM pile material as obtained from an oedometer test; $m_{v,p}/m_{v,c}$ is the ratio of the coefficient of volume change of the DMM pile and the surrounding clay; $n = (D_e/d_p)$ is the ratio of the equivalent diameter of the unit cell to the diameter of the pile (where $D_e = 1{\cdot}03S$ and $1{\cdot}13S$ corresponding to triangular and square patterns of the piles, respectively, S is the centre-to-centre spacing of the piles, and d_p is the diameter of pile); H_p is the effective longest drainage path of the consolidating soil–cement pile; and t is the time when a particular degree of consolidation is desired.

The actual load transfer mechanism is neither equal strain nor equal stress; however, it must fall within these two extreme conditions. The actual average degree of consolidation can better be estimated by applying the appropriate weighting factor to each average degree of consolidation from the two extreme conditions. Thus, the actual average degree of consolidation of the improved ground, $\overline{U}$, will be predicted using the following relationship

$$\overline{U} = \alpha_\varepsilon(\overline{U}_{v,\varepsilon}) + \alpha_\sigma(\overline{U}_{v,\sigma}) \quad (3)$$

where α_ε and α_σ are the weighting factors of the average degree of consolidation corresponding to equal strain and equal stress conditions, respectively; $\overline{U}_{v,\varepsilon}$ is the average degree of consolidation under equal strain condition calculated using the standard solution (or chart) or to any approximate solutions (e.g., Sivaram and Swamee, 1977) of a one-dimensional consolidation equation with the time factor, $T_{v\varepsilon}$, given in equation (2); and $\overline{U}_{v,\sigma}$ is the average degree of consolidation under equal stress condition calculated using the time factor, $T_{v\sigma}$, given in equation (1). Obviously, the sum of these two weighting factors, α_ε and α_σ, must be equal to unity.

Input soil parameters for the analytical model

The consolidation parameters as well as the strength parameters of soil–cement piles used in the back analyses were estimated based on the test piles, which were installed few meters away from the embankment. Petchgate *et al.* (2003) reported the following properties of the tested soil–cement piles: water content = 160%, $\gamma_{wet} = 12{\cdot}8\ kN/m^3$; $q_u = 300 - 700$ kPa and $E_{50} = 60\,000$–$120\,000$ kPa. From laboratory testing, the specific gravity of the cement-admixed clay composing the pile is approximately 2·65. Accordingly, the after-curing void ratio of cement-admixed clay composing the soil–cement pile can be obtained as 4·3, which is almost twice the void ratio of the natural clay. At this magnitude of after-curing void ratio of soil–cement piles, the coefficient of vertical permeability, $K_{v,p}$, ranges from 150 to 200×10^{-10} m/s and the corresponding coefficient of consolidation, $C_{v,p}$, ranges from 200 to 400 m^2/year (Lorenzo and Bergado, 2003b). In addition, for the surrounding clay, the coefficient of vertical permeability, $K_{v,c}$, ranges from 3 to 6×10^{-10} m/s and the corresponding coefficient of consolidation, $C_{v,c}$, ranges from 1 to 3 m^2/year (Lorenzo and Bergado, 2003b).

Soil models and parameters used in numerical analysis

In the FE analysis, PLAXIS software version 7 developed by Brinkgreve *et al*. (1996) was used. The FE model of the MSE embankment consisted of the hexagonal wire mesh reinforcement, soil-to-reinforcement interaction and concrete facing elements and their connections. The six-node triangular FE (Fig. 11) was used in the foundation soil. The soft soil model (SSM), which is similar to the cam clay model, was used to model the behaviour of a soft clay foundation, and the hardening soil model (HSM) in PLAXIS was used for the medium clay and over-consolidated clay as well as the embankment fill. In addition, the Mohr–Coulomb model (MCM) was used for the soil–cement pile. The soil–cement piles, each having 0·5 m diameter and arranged at 1·5 m spacing in square pattern, were transformed into an equivalent continuous wall of the same area directed in out of plane.

The hexagonal wire mesh reinforcements are flexible materials capable only of resisting tensile stresses, and in PLAXIS software this type of material is modelled as 'geotextile'. A 'geotextile' element needs only an axial stiffness, AE, where A is the cross-sectional area per unit width in out of plane and E is the modulus of elasticity of the material. To simulate the soil interaction between the interfaces of the reinforcements, 'interface' elements are placed at both faces of each reinforcement layer. A three-node interface element in PLAXIS was used in conjunction with a six-node triangular finite element. An 'interface' element requires a strength reduction factor, R_{inter}, which is the fraction of the surrounding soil strengths (cohesion and/or friction) that effectively mobilised at the interface.

Each of the concrete-facing panels, which are held by the hexagonal wire mesh reinforcements, at the vertical face of the embankment was modelled as 'beam' element. Furthermore, the concrete facing-to-facing connection was idealised to behave as a hinge. In addition to axial stiffness, AE, the 'beam' element requires flexural stiffness, EI, where 'I' is the centroidal moment of inertia of the cross-section about the out-of-plane axis per unit width of the concrete facing.

The SSM is a cam-clay type model developed by Brinkgreve *et al*. (1996). The soil parameters used for this model are given in Table 1. The drained modulus was estimated using the correlations of Parnploy (1985). The dilatancy angle (ψ) and Poisson's ratio (ν) were assumed to

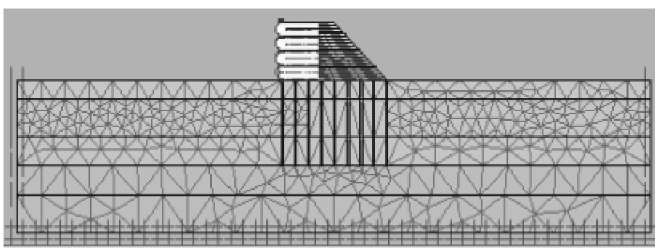

Fig. 11. Portion of the numerical model of the test embankment

Table 1. Soil models and parameters used in FE simulation

Materials	Description	Model	γ: kN/m³	c_u: kPa	OCR	c': kPa	ϕ': deg	λ^*	κ^*	E'_{ref}: kPa	ν'	k: m/day
Subsoil												
0–2·5 m	Weathered crust	HSM	16	16	9	1–8	23			2500	0·25	0·00005
2·5–9 m	Soft clay	SSM	14·7	12	1·5	0	23	0·12–0·16	0·02–0·03	350		0·00005–0·00015
9–12 m	Medium stiff clay	HSM	15·5	60	2·0	1–8	23			3000	0·25	0·00005
12–16 m	Stiff clay	HSM	17·0	100	2·6	1–10	23			4700	0·25	0·00001
Embankment	Silty sand	MCM	20			1–5	30			5600	0·30	Drain
Hexagonal wire mesh	Reinforcement	EM	AE = 900 kN/m; with interface elements at both sides; R_{inter} = 0·5									
Concrete facing	Concrete facing elements	EM	AE = 1200000 kN/m; EI = 270 kN-m²/m									
Soil–cement pile	DMM pile	MCM	15	300	—	300	28–30	—	—	13500–17000	0·33	$K_{v,p}/K_{v,c} = 30$

SSM: soft soil model; HSM: hardening soil model; MCM: Mohr–Coulomb model; EM: elastic model; $\lambda^* = C_c/[2{\cdot}303(1 + e_o)]$; $\kappa^* = C_s/[2{\cdot}303(1 + e_o)]$

be 0 and 0·25 respectively, assuming drained conditions. The drained friction angle, ϕ', was taken from the work of Balasubramaniam *et al*. (1978). The modified compression index (λ^*) and modified swelling index (κ^*) were determined from the work of Hassan (1993) and Lorenzo (2001). The overconsolidation ratio (OCR) was estimated following the empirical correlation given by Mayne and Mitchell (1988). Vertical permeability, k_v, was obtained from Lorenzo (2001) and Lorenzo and Bergado (2003b), with an assumption that field permeability is twice the laboratory permeability. Furthermore, the horizontal permeability was assumed to be twice the corresponding vertical permeability (Lorenzo, 2001).

The HSM is an elasto-plastic type of hyperbolic model, formulated in the framework of friction hardening plasticity. This second-order model can be used to simulate the behaviour of stiffer soils, such as overconsolidated clays, sand and gravel (Brinkgreve *et al*., 1996). The failure criteria of these models are similar to that of MCM; however, it differs from MCM with the use of stress-level-dependent drained modulus, E_{50}, which is given as follows

$$E_{50} = E_{50}^{\mathrm{ref}}\left(\frac{c'\cot\phi - \sigma_3'}{c'\cot\phi + p^{\mathrm{ref}}}\right)^m \tag{4}$$

where $E^{\mathrm{ref}}{}_{50}$ is the referenced secant stiffness modulus corresponding to referenced confining pressure p^{ref} of 100 kPa; E_{50} is the actual stiffness of the soil, which is dependent on the minor principal stress, σ_3'; m is the power for stress-level dependency of stiffness, which ranges from 0·5 to 1, and can be taken as 0·5 for sand and silts (Janbu, 1963). In this analysis, m was assumed to be 0·5 for the weathered clay, medium-stiff clay and stiff clay layers respectively. The drained friction angles are estimated from the work of Bjerrum and Simons (1960).

The MCM was selected to model the behaviour of soil–cement piles. The MCM assumed a fixed yield surface in a principal stress space, which is fully defined by model parameters. In any stress state that is below the yield surface, the behaviour is purely elastic and all strains are reversible, hence similar to the elastic model. The parameters assigned for the soil–cement piles are also shown in Table 1. The drained cohesion, c', was taken from laboratory test of Uddin (1995). The drained modulus, E', and the vertical permeability of the DMM pile of 30 times that of the surrounding soil were based from the back analysis conducted by Lorenzo (2001) of the Bangna–Bangpakong Highway, Bangkok, Thailand, which was improved with DMM cement piles.

The MCM was also used to model the silty sand backfill of the proposed MSE embankment. The soil parameters utilised in the analysis are also given in Table 1.

Results of back analysis

Results from analytical back-analysis

Figures 12 and 13 show the predicted settlement–time plots together with the corresponding measured settlement–time plots from settlement plates S1 versus S5, and S11 versus S15, respectively (refer to Fig. 2(a) for their locations). Two adjacent settlement plates are paired, one on deep jet mixing (DJM) pile and the other on the adjacent clay in-between DJM. In the analysis, the immediate settlement and the consolidation settlement were first obtained by trial until the actual settlement just after embankment construction and one year after construction (last observed data) agreed

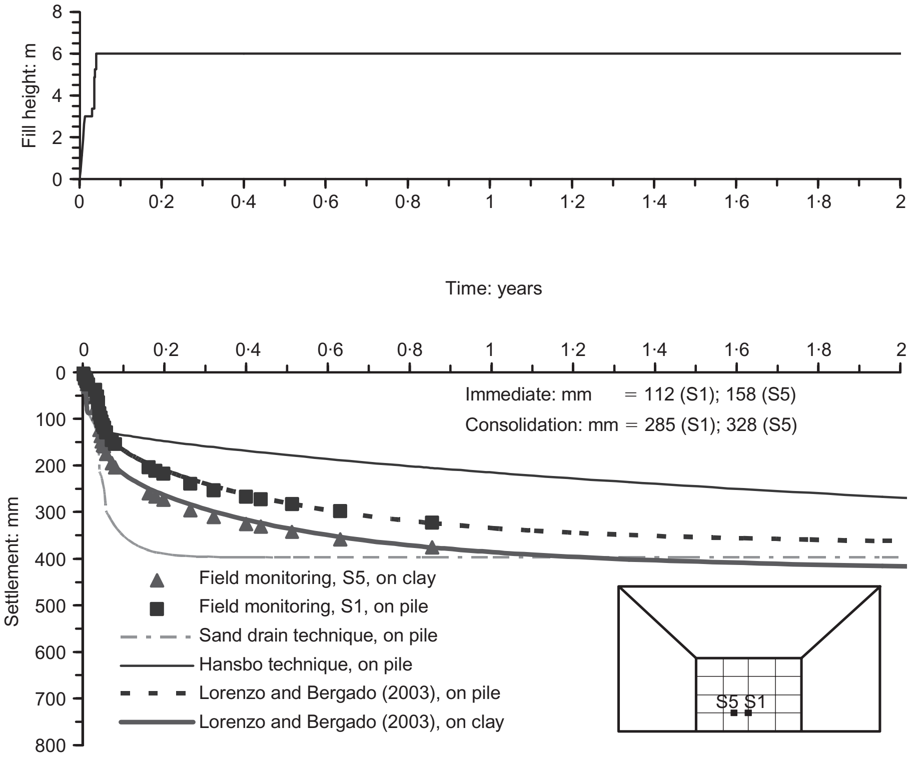

Fig. 12. Comparison between field data and back analyses (S1 versus S5)

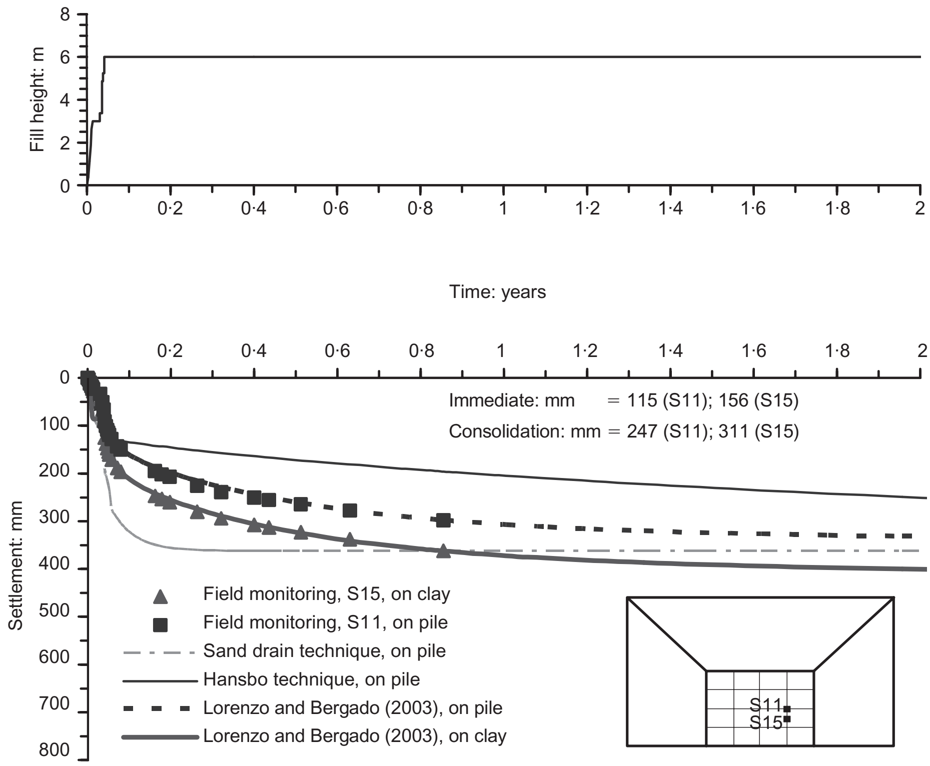

Fig. 13. Comparison between field data and back analyses (S11 versus S15)

to the predicted or projected ones. The behaviour of the settlement against time reflects the consolidation properties such as permeability ratio ($k_{v,p}/k_{v,c}$), compressibility ratio ($m_{v,p}/m_{v,c}$), and the coefficient of consolidation of the deep mixing pile ($c_{v,p}$).

The good agreement between the measured and the predicted settlement-time plots shown in Figs 12 and 13 were obtained using the coefficient of consolidation of the pile ($c_{v,p}$) of 800 m^2/year and coefficient of consolidation of surrounding clay ($c_{v,c}$) of 2·0 m^2/year. Bergado *et al.* (1999) and Lorenzo and Bergado (2003a) also utilised coefficient of consolidation of surrounding clay ($c_{v,c}$) of 2·0 for the back-analysis of Bangna–Bangpakong Highway embankment, which was also improved by DMM. Moreover, the compressibility ratio ($m_{v,p}/m_{v,c}$) of 0·10 was used, which also confirmed the back analysis of another case study done previously by Lorenzo and Bergado (2003a). Consequently, the permeability ratio ($k_{v,p}/k_{v,c}$) was derived as 40, which is twice that obtained by Bergado *et al.* (1999) and Lorenzo and Bergado (2003a) for the Bangna–Bangpakong Highway embankment. The higher permeability ratio obtained from this study compared with the previous case of Bangna–Bangpakong Highway embankment could be attributed to the different methods of mixing applied. The deep mixing piles supporting the reinforcement embankment mentioned in this paper were installed by the jet mixing method with cement slurry employing a jet pressure of 20 MPa, while those supporting the Bangna–Bangpakong Highway embankment were installed by the mechanical mixing method with cement slurry as reported by Bergado *et al.* (1999). It has been found from the laboratory investigation that the increase in mixing water content corresponded with an equivalent increase in the after-curing void ratio and, hence, the coefficient of permeability and consolidation of the resulting cement-admixed clay (Lorenzo and Bergado, 2003b; Lorenzo and Bergado, 2004). In the case of the present test embankment, therefore, the higher water content deliberately added into the soil during jet mixing must have affected the higher coefficient of consolidation of the resulting soil–cement piles compared with those from Bangna–Bangpakong Highway embankment, which were installed by a mechanical mixing method.

Furthermore, the weighting factors of the average degree of consolidation, α_ε and α_σ, as mentioned in equation (3) corresponding to 'equal strain' and 'equal stress' conditions, respectively, that were utilised in the analysis and simulated closely to the actual rate of settlement of the improved ground, are 80% for equal strain and 20% for equal stress. This means that at any time the overall degree of consolidation of the improved ground was taken to be equal to 80% of the average degree of consolidation under equal strain condition plus 20% of the average degree of consolidation under equal stress condition.

Moreover, the corresponding settlement–time curves from the existing methods, such as Hansbo (1979) for prefabricated vertical drain and Barron (1948) for sand drains, of predicting the consolidation settlement using unit cell technique are also presented in Figs 12 and 13. Each of these figures shows that the sand drain technique overestimated the rate of settlement of soil–cement pile improved ground. It follows, therefore, that soil–cement pile cannot behave exactly as sand drain. This is because, owing to the very high permeability of sand compared with soil–cement pile, the consolidation process of sand can occur very quickly compared with that of the soil–cement pile. On the other hand, the use of Hansbo's (1979) technique, which assumed that soil–cement pile could be converted to an equivalent vertical drain, underestimated the actual settlement. Lorenzo and Bergado (2003a) presented the following reasons. First, owing to the fact that the discharge capacity of the soil–cement pile is quite small compared with that of actual prefabricated vertical drain, significant time is required to discharge the excess pore water in the soil–cement pile. Second, very different boundary conditions must be met for soil–cement pile unit cells versus prefabricated vertical drain unit cells. While the prefabricated vertical drain is considered to be a drain within the unit cell, the pile in a soil–cement unit cell cannot be considered as a drain owing to its lower permeability and smaller capacity to discharge water than the prefabricated vertical drain. This means that, at any time, the excess pore water pressure at any depth of soil–cement pile cannot be assumed as zero: it is assumed as zero in the prefabricated vertical drain analysis. Moreover, the consolidation process of the pile in a soil–cement pile unit cell is quite quantifiable and cannot be assumed to be as 'quick' as either sand drains or prefabricated vertical drains.

Significantly, the good agreement of the predicted settlement–time plots, predicted using the method of Lorenzo and Bergado (2003a), compared with the measured ones not only confirms the previous findings of Lorenzo and Bergado (2003a) but also indicates the suitability of the method to deep mixing improved ground for which it was designed.

Results from FE simulation

Figure 14 shows the displacement vectors at the bottom of the test embankment as obtained from the FE simulation. The predicted consolidation settlements of the adjacent clay surrounding the pile at points C and D (Fig. 14) yielded good agreement with the corresponding measured data obtained from the closest surface settlement plates S5 and S6 as demonstrated in Fig. 15. This good agreement was achieved when the permeability ratio, $K_{v,p}/K_{v,c} = 30$, was used in the FE simulation, which is 1·5 times that obtained by Bergado *et al.* (1999) and Lorenzo and Bergado (2003a) from the case of the Bangna–Bangpakong Highway embankment, which was founded on cement deep mixing piles installed by the slurry mechanical mixing method.

As discussed earlier, the higher permeability ratio obtained from this study compared with the previous case of the Bangna–Bangpakong Highway embankment could be attributed to the method of mixing applied in the present test embankment. In the case of the latter, the higher water content deliberately added into the soil during jet mixing must have increased the after-curing void ratio and, hence, the coefficients of permeability and consolidation of the resulting deep mixing piles (Lorenzo and Bergado, 2003b; Lorenzo and Bergado, 2004). Furthermore, the results from FE simulation also confirmed that the deep mixing piles not only reduced the magnitude of total settlement but also accelerated the consolidation of the improved ground.

Conclusions

(*a*) The deep mixing improvement in the soft clay foundation has effectively reduced the settlement of the reinforced test embankment by 70%. Just after the embankment construction, the settlement of the improved ground already amounted to 40% of the total settlement.

(*b*) The local differential settlement between piles and the adjacent surrounding soil amounted to 25 to 60 mm, which was approximately 8 to 20% of the average settlement. The local differential settlement, however, was not obvious at the top surface of the embankment

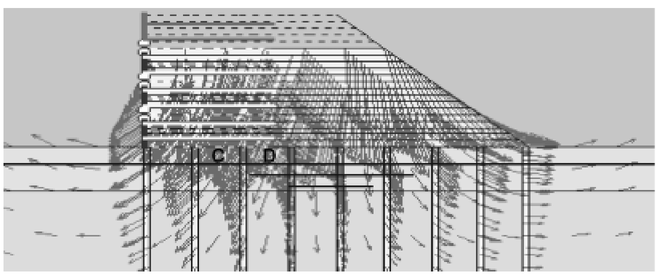

Fig. 14. Total displacement vector

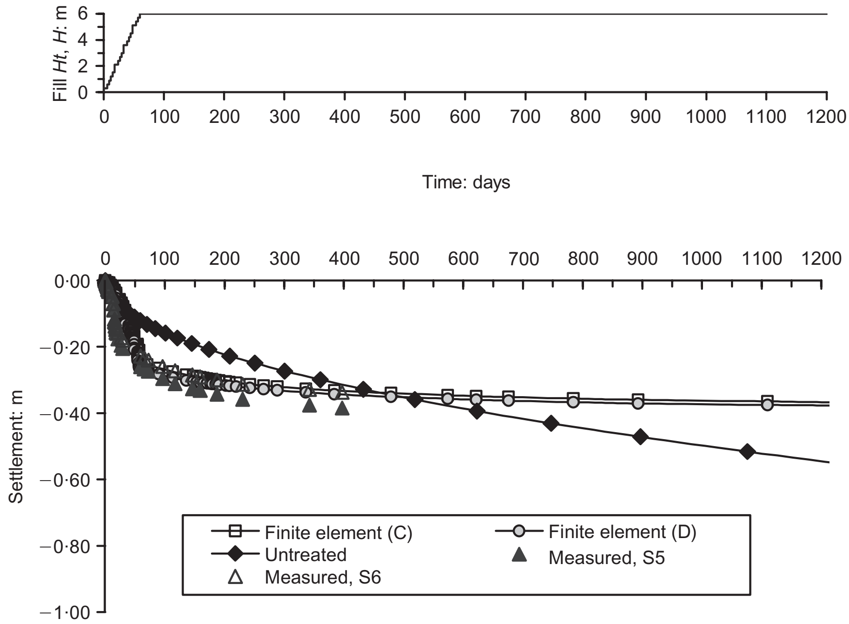

Fig. 15. Settlement–time plot from finite element simulation

owing to the combined effect of compaction as well as reinforcement stiffness and arching of the reinforced soil.

(*c*) The jet mixing method can create soil–cement piles with higher after-curing void ratio and, hence, higher coefficients of permeability and consolidation. The higher permeability ratios, $K_{v,p}/K_{v,c}$, of 30 and 40 were confirmed from numerical and analytical analyses, respectively. In addition, in the analytical back analysis the following parameters were obtained: compressibility ratio ($m_{v,p}/m_{v,c}$) of 0·10; coefficients of consolidation of the deep mixing pile ($c_{v,p}$) and of the surrounding clay ($c_{v,c}$) of 800 and 2·0 m^2/year, respectively.

(*d*) The effectiveness of DJM in improving thick deposit of soft clay for foundation of reinforced embankment has been confirmed as follows: (*i*) reduce the compressibility of the improved foundation ; and (*ii*) increase the rate of consolidation of the improved foundation.

References

Asaoka A. (1978) Observational procedure of settlement prediction. *Soils and Foundations*, **18**, No. 4, 53–66.

Balasubramaniam A. S., Huang Z. M., Uddin W., Chaudhry A. R. and Li Y. G. (1978) Critical state parameters and peak stress envelopes for Bangkok clays. *Quarterly Journal of Engineering Geology*, **11**, 219–232.

Barron R. A. (1948) Consolidation of fine-grained soils by sand drain wells. *Transactions of the American Society of Civil Engineers*, **113**, 718–724.

Bergado D. T., Lorenzo G. A. and Chai X. C. (2002) Construction behavior of hexagonal wire reinforced embankment on deep jet grouted soil-cement piles improved soft Bangkok clay. *Proceedings of the Symposium of Ground Improvement and Geosynthetics*, KMUTT, Bangkok, Thailand, pp. 115–124.

Bergado D. T. and Lorenzo G. A. (2003) Behavior of reinforced embankment on soft ground with and without jet grouted soil-cement piles (in TC9 Lecture). *Proceedings of the 12th Asian Regional Conference on Soil Mechanics and Geotechnical Engineering*, Singapore, pp. 1311–1316.

Bergado D. T., Ruenkrairergsa T., Taesiri Y. and Balasubramaniam A. S. (1999) Deep soil mixing used to reduce embankment settlement. *Ground Improvement*, **3**, 145–162.

Bjerrum L. and Simons N. E. (1960) Comparison of shear strength characteristics of normally consolidated clay. *ASCE Proceedings, Research Conference on Shear Strength of Cohesive Soil*, American Society of Civil Engineers, Reston, pp. 711–726.

Brinkgreve R. B. J., Vermeer P. A. and Balkema A. A. (1996) *PLAXIS, Finite Element Code for Soils and Rock (Version 7)* (ed. R. B. J. Netherland) A. A. Balkema, Rotterdam.

Duangchan T. (2002) *Measured Versus Predicted Settlements and Pullout Capacity in Full Scale Reinforced Embankment on DJM Piles*. MEng thesis, Asian Institute of Technology, Thailand.

Hansbo S. (1979) Consolidation of clay by bandshaped prefabricated drains. *Ground Engineering*, **12**, No. 5, 16–25.

Hassan I. S. (1993) *Consolidation Behavior of Bangkok Clay under Constant Rate of Strain Consolidometer*. MEng Thesis No. GT-92-3, Asian Institute of Technology, Bangkok, Thailand.

Janbu J. (1963) Soil compressibility as determined by oedometer and triaxial tests. *Proceedings of European Conference on Soil Mechanics and Foundation Engineering*, Wiessbaden, Vol. 1, pp. 19–25.

Kamon M and Bergado D. T. (1991) Ground improvement techniques. *Proceedings of the 9th Asian Regional Conference on Soil Mechanics and Foundation Engineering*, Bangkok, **2**, 526–546.

Kamon M. (1996) Effect of grouting and DMM on big construction projects in Japan. *Proceedings of IS-Tokyo '96/The Second International Conference on Ground Improvement and Geosystems*, Tokyo, Vol. 2, pp. 807–823.

Lorenzo G. A. (2001) *A New Compressibility Model and Finite Element Simulation on Deep Mixing Method (DMM) Applications*. MEng thesis, Asian Institute of Technology, Thailand.

Lorenzo G. A. and Bergado D. T. (2003a) New consolidation equation for soil–cement pile improved ground. *Canadian Geotechnical Journal*, **40**, No. 2, 265–275.

Lorenzo G. A. and Bergado D. T. (2003b) Fundamentals of high water content deep mixing piles. *Proceedings of the International Symposium 2003 on Soil/Ground Improvement and Geosynthetics in Waste Containment and Erosion Control Applications*, Asian Institute of Technology, Thailand, pp. 155–174.

Lorenzo G. A. and Bergado D. T. (2004) Fundamental parameters of cement-admixed clay – new approach. *Journal of Geotechnical and Geoenvironmental Engineering, ASCE*, **130**, No. 10, 1042–1050.

Mayne P. W. and Mitchell J. K. (1988) Profiling of overconsolidation ratio in clays by field vane. *Canadian Geotechnical Journal*, **25**, No. 1, 150–158

Parnploy U. (1985) *Deformation analysis and settlement prediction of Bangna–Bangpakong Highway (section 1)*. MEng Thesis, Asian Institute of Technology, Bangkok, Thailand.

Petchgate K., Jongpradist P. and Panmanajareonphol S. (2003) Field pile load test of soil–cement column in soft clay. *Proceedings of the International Symposium 2003 on Soil/Ground Improve-*

ment and Geosynthetics in Waste Containment and Erosion Control Applications, Asian Institute of Technology, Thailand, pp. 175–184.

Porbaha A. (1998). State of the art in deep mixing technology. Part I: Basic concepts and overview. *Ground Improvement*, **2**, No. 2, 81–92.

Sivaram B. and Swamee, P. (1977) A computational method for consolidation coefficient. *Soil and Foundations*, **17**, No. 12, 48–52.

Uddin M. K. (1995) *Strength and Deformation Characteristics of Cement-Treated Bangkok Clay*. DEng Dissertation No. GT-94-1, Asian Institute of Technology, Bangkok, Thailand.

Discussion contributions on this paper should reach the editor by 2 April 2007